MULTIFREQUENCY OBSERVATIONS OF BL LACERTAE IN 1988

N. Kawai and M. Matsuoka
The Institute of Physical and Chemical Research, 2-1 Hirosawa, Wako, Saitama 351-01, Japan

J. N. Bregman, H. D. Aller, M. F. Aller, and P. A. Hughes
Department of Astronomy, University of Michigan, Ann Arbor, MI 48109–1090

S. A. Balbus
Astronomy Department, University of Virginia, P.O. Box 3818, University Station, Charlottesville, VA 22903

T. J. Balonek
Department of Physics and Astronomy, Colgate University, Hamilton, NY 13346

K. C. Chambers
Leiden Observatory, Nielsbohrweg 2, 2300 RA Leiden, Netherlands

R. E. S. Clegg
Royal Greenwich Observatory, Madingley Road, Cambridge CB3 0EZ, England, UK

S. D. Clements, R. J. Leacock, and A. G. Smith
Astronomy Department, University of Florida, SSRB 211, Gainesville, FL 32611

J. S. Miller
Lick Observatory, University of California, Santa Cruz, CA 95064

M. Hereld
Astronomy and Astrophysics Center, University of Chicago, 5640 S. Ellis Avenue, Chicago, IL 60637

M. G. Hoare
Department of Astrophysics, University of Oxford, Nuclear Physics Laboratory, Keble Road, Oxford OX1 3RH, England, UK

V. A. Hughes
Astronomy Group, Department of Physics, Queens University, Kingston, ON, K7L 3N6 Canada

G. K. Miley
Sterrewacht, Postbus 9513, 2300 RA Leiden, Netherlands

G. H. Moriarty-Schieven
Jet Propulsion Laboratory, MS 169-506, California Institute of Technology, 4800 Oak Grove Drive, Pasadena, CA 91109

K. Matthews and G. Neugebauer
Palomar Observatory, California Institute of Technology, Pasadena, CA 91125

T. Ohashi
Physics Department, University of Tokyo, 3-1 Hongo 7-chome, Bunkyo-ku, Tokyo 113, Japan

P. F. Roche
Royal Observatory Edinburgh, Blackford Hill, Edinburgh EH9 3HJ, Scotland, UK

H. A. Thronson
Department of Physics and Astronomy, University of Wyoming, Box 3905, Laramie, WY 82071

E. Valtaoja and H. Terasranta
Metsahovi Radio Research Station, Helsinki University of Technology, Otakaari 5 A, SF-02150 Espoo, Finland

J. R. Webb
Department of Physics, Florida International University, Tamiami Campus/University Park, Miami, FL 33199

AND

R. Goodrich, B. J. Wills, and D. Wills
Astronomy Department, University of Texas, RLM 15.308, Austin, TX 78712

ABSTRACT

Simultaneous multiwavelength observations of BL Lacertae were performed on two occasions separated by 1 month in 1988 June and July, covering the radio, submillimeter, infrared, optical, ultraviolet, and X-ray wave bands. In the wide-band photon spectra, the X-ray flux lies clearly above the extension of radio-ultraviolet continuum as expected. The slope of the X-ray spectra is significantly flatter than that at optical-ultraviolet regimes, and its spectral index 0.7–1.0 corresponds to the slope at submillimeter band. Comparison with earlier observations, in fact, indicates that the X-ray flux is correlated with the submillimeter band, and not with the others, and supports the SSC model.

Subject headings: BL Lacertae objects — infrared: sources — radiation mechanisms — radio sources: variable — X-rays: spectra

1. INTRODUCTION

The study of the BL Lacertae class of objects has proven extremely valuable in developing an understanding of the continuum emission processes in active galactic nuclei (AGNs). The lack of emission lines, blue bumps, and galaxy features in luminous BL Lacertae objects permit us to view the non-thermal continuum directly and without confusion. While many advances have been made from VLBI programs and multiwavelength observations of the continuum from the radio through the X-ray region, the X-ray emission mechanism in many objects remains unclear (see Bregman, Maraschi, & Urry 1987; Urry 1988).

In many of the X-ray bright BL Lacertae objects, the X-ray emission appears to be a smooth extension of the optical-ultraviolet emission, suggesting that it too is produced by the synchrotron process (examples are PKS 2155−304, Ohashi et al. 1989; Mrk 421, Makino et al. 1987). However, for some sources the X-ray emission lies above an extrapolation of the optical-ultraviolet continuum and has a different slope. In objects such as these, of which BL Lacertae is one of the brightest examples, the X-ray emission is probably produced by a process distinct from the synchrotron mechanism that produces the radio through ultraviolet emission. This paper addresses the origin of the X-ray emission from BL Lacertae by performing an observational test that can distinguish between two competing models.

One of the leading models for the production of X-ray emission is the well-developed synchrotron-Compton model (Jones, O'Dell, & Stein 1974; Gould 1979) in which photons in the radio through infrared regions are scattered by relativistic electrons ($\gamma \sim 30$–10^4) into the X-ray region. This model predicts (1) that the spectral slope of the synchrotron continuum (the seed photons) should match that of the Compton-scattered continuum and (2) that the seed and scattered photons should vary together.

In an alternative model, the pair-cascade model (Guilbert, Fabian, & Rees 1983; Svensson 1987), the X-rays are produced in a much more compact region, presumably near the very center of the "central engine." Gamma-ray photons ($E > m_e c^2$) are assumed to be created in a region in which the density of soft photons (optical-ultraviolet) is so large that the optical depth to photon scattering exceeds unity. Photon scattering of the gamma-rays with the soft photons leads to electron-positron pairs and following a wide assortment of creation, destruction and scattering processes, optical, and ultraviolet photons are scattered into the X-ray region. The spectral slope of this X-ray emission, expected to lie in the range $-0.5 \sim -1.5$, is determined by opacity effects, and can be

quite different from the optical-ultraviolet continuum. Unlike the synchrotron-Compton model, variation of the X-rays can be rapid and would be expected to follow changes in the optical-ultraviolet continuum, assuming that other model parameters remain unchanged. Because the expected behavior of the two models are distinct, it should be possible to perform a critical observational test.

One of the objects best suited for testing the origin of the X-ray emission is BL Lacertae (2200+420), the archetype of its field, lying in a giant elliptical galaxy at a redshift of 0.0688 (Miller, French, & Hawley 1978). Not only is the X-ray emission separate from the radio-ultraviolet emission, it is bright enough to be detected over a broad range of wavelengths with current instruments; it is the only BL Lacertae object with these properties that can be detected by *Ginga*. In order to identify the seed photons in the synchrotron-Compton model, it is necessary to match the spectral slope in the X-ray region to that in the radio-infrared region. A unique matching is possible with BL Lacertae because the spectral slope increases monotonically between the radio and ultraviolet regions.

In a recent study of BL Lacertae, Bregman et al. (1990) obtained a series of four multifrequency spectra including data from the radio to X-ray region. Using the two multifrequency spectra with X-ray measurements, it was found that the X-ray flux density changed in the same sense as the radio-infrared continuum but in the opposite sense from the optical-ultraviolet continuum. The X-ray spectral slope, as determined by the IPC to MPC measurements on the *Einstein Observatory*, appeared to be similar to the infrared continuum. These results, if representative of BL Lacertae, provide the strongest evidence to date in support of the synchrotron-Compton model.

Here we present additional multifrequency observations of BL Lacertae in an effort to study more deeply the previously reported behavior and to further test the proposed X-ray emission mechanisms. Simultaneous measurements from the radio through the X-ray wavebands are used to define two time-frozen spectra. Unlike earlier observations, the use of the *Ginga* X-ray satellite permit an accurate determination of the X-ray spectral slope with a single instrument and up to higher energies (30 keV). The characteristics of these observations (§ 2) are compared to previous observations as well as to the model predictions (§ 3).

2. OBSERVATIONS AND DATA

Multifrequency spectra were obtained on two dates: 1988 June 15 and 1988 July 17. The participating observers and the facilities are listed in Table 1. The observed data are shown in

TABLE 1
OBSERVERS OF THE MULTIWAVELENGTH CAMPAIGN FOR BL LACERTAE, 1988 JUNE/JULY

Band	Observer	Facility or Institution
4.8, 8.0, 14.5, GHz	Aller, Aller, & Hughes	University of Michigan Radio Observatory
90 GHz	Balonek	NRAO
22–87 GHz	Valtaoja and Terasranta	Metsahovi Radio Research Station
1 mm	Hughes and Moriarty-Schieven	JCMT
1 mm	Hoare, Clegg, and Roche	JCMT
IR	Chambers and Miley	UKIRT
IR	Hereld and Thronson	University of Wyoming Infrared Telescope
IR	Matthews and Neugebauer	Palomar Observatory
Optical	Clements, Webb, Smith, and Leacock	Rosemary Hill Observatory, University of Florida
Optical	Miller and Goodrich	Lick Observatory
Optical	Wills and Wills	McDonald Observatory
UV	Bregman and Balbus	*IUE*
X-ray	Kawai, Matsuoka, and Ohashi	*Ginga*

TABLE 2
MULTIFREQUENCY DATA FOR BL LACERTAE, 1988 JUNE/JULY

Observers	Date (1988)	Region	log ν(Hz)	Flux	log $F\nu$[a]	log σ
Kawai, Matsuoka,	Jun 15	2[b]	17.680	7.76E − 30[c]	−29.11	0.01
and Ohashi		3	17.861	5.88E − 30	−29.23	0.01
		5	18.082	4.04E − 30	−29.39	0.02
		6	18.160	3.55E − 30	−29.45	0.02
		8	18.287	2.91E − 30	−29.54	0.02
		15	18.552	1.91E − 30	−29.72	0.04
	Jul 17	2	17.680	6.03E − 30	−29.22	0.02
		3	17.861	4.85E − 30	−29.31	0.02
		5	18.082	2.96E − 30	−29.53	0.03
		6	18.160	2.40E − 30	−29.62	0.03
		8	18.287	1.77E − 30	−29.75	0.04
		15	18.552	8.95E − 31	−30.05	0.12
Bregman and Balbus	Jun 15	2500[d]	15.079	9.95E − 16[e]	−25.78	0.06
		2650	15.054	7.60E − 16	−25.93	0.03
		2750	15.038	7.90E − 16	−25.92	0.02
		2850	15.022	7.70E − 16	−25.95	0.02
		2950	15.007	1.00E − 15	−25.82	0.02
		3050	14.993	1.20E − 15	−25.75	0.03
	Jul 17	2550	15.071	1.20E − 15	−25.72	0.03
		2650	15.054	7.00E − 16	−25.97	0.03
		2750	15.038	7.50E − 16	−25.95	0.02
		2850	15.022	7.80E − 16	−25.94	0.02
		2950	15.007	1.10E − 15	−25.78	0.03
		3050	14.993	7.20E − 16	−25.97	0.06
Miller and Goodrich	Jun 15	3500	14.933	9.16[f]	−25.82	0.04
		4000	14.875	11.47	−25.66	0.04
		4500	14.824	12.75	−25.57	0.04
		5000	14.778	15.02	−25.46	0.04
		5500	14.737	16.95	−25.38	0.04
		6000	14.699	18.61	−25.30	0.04
Clements, Webb, Smith,	Jun 15	3600	14.921	16.48[g]	−25.75	0.04
and Leacock		4400	14.834	16.54	−25.45	0.03
		5500	14.737	15.27	−25.16	0.02
	Jul 17	3600	14.921	16.55	−25.78	0.08
		4400	14.834	16.65	−25.50	0.04
		5500	14.737	15.33	−25.19	0.03
Chambers and Miley	Jun 14	1.25[h]	14.380	12.50[i]	−24.70	0.06
		2.20	14.135	10.90	−24.50	0.06
Hereld and Thronson	Jun 15	1.25	14.380	12.58	−24.74	0.02
	8–9 hr UT	1.65	14.260	11.65	−24.61	0.02
		2.20	14.135	10.69	−24.44	0.02
Matthews	Jul 1	1.27	14.373	22.00[j]	−24.56	0.03
and Neugebauer		1.65	14.260	31.00	−24.45	0.03
		2.20	14.135	44.00	−24.32	0.03
		3.70	13.909	61.00	−24.21	0.03
		10.10	13.473	140.00	−23.85	0.07
Hoare, Clegg, and Roche	Jun 8	800	11.574	2.16[k]	−22.67	0.04
	17:00 UT	1100	11.436	1.99	−22.70	0.04
Hughes and	Jul 19	450	11.824	1.32	−22.88	0.18
Moriarty-Schieven	12:30 UT	800	11.574	1.65	−22.78	0.02
		1100	11.436	1.88	−22.73	0.02
Balonek	Jun 15	90[l]	10.952	3.20	−22.49	0.00
Valtaoja and Terasranta	Jun 12	87	10.940	2.46	−22.61	0.03
	Jun 15	37	10.568	3.49	−22.46	0.02
	Jun 15	22	10.342	4.04	−22.39	0.02
		87	10.940	2.46	−22.61	0.03
	Jul 11	37	10.568	3.36	−22.47	0.01
	Jul 10	22	10.342	3.42	−22.47	0.02
Aller, Aller, and Hughes	Jun 15	14.5	10.161	3.90	−22.41	0.003
		8.0	9.903	4.17	−22.38	0.004
		4.8	9.681	3.92	−22.41	0.004
	Jul 17	14.5	10.161	3.90	−22.41	0.004
		8.0	9.903	4.31	−22.37	0.009
		4.8	9.681	4.12	−22.39	0.011
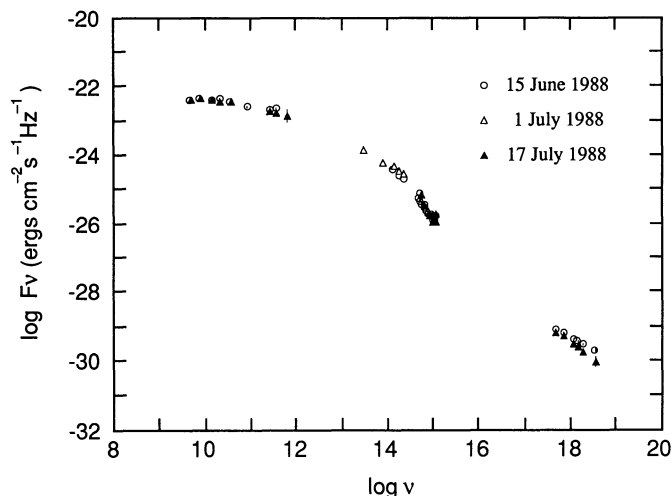
FIG. 1.—Wide-band multiwavelength spectra of BL Lacertae

TABLE 3

WIDE-BAND X-RAY FLUX[a]

Energy Range (keV)	1988 June 15	1988 July 16
1.7–5.8	2.27 ± 0.06	1.89 ± 0.07
5.8–9.8	0.92 ± 0.04	0.56 ± 0.05
9.8–19.6	0.52 ± 0.04	0.22 ± 0.05
1.7–19.6	3.71 ± 0.08	2.68 ± 0.10

NOTE.—The errors for count rates are 1 σ Poissonian.

[a] Count s^{-1} for 4000 cm^2.

Table 2 and Figure 1. Because of the large number of observatories and instruments used, the details of each observation are not given except for the X-ray observations, for which the spectrum was measured in a higher energy range up to 20 keV for the first time.

The correction for reddening in infrared, optical and ultraviolet observations is described in the earlier paper of BL Lacertae observations (Bregman et al. 1990).

2.1. X-Ray Observations

BL Lacertae was observed with the large area proportional counters (LAC) on board the *Ginga* satellite (Turner et al. 1989) on 1988 June 15 and 1988 July 17, dates chosen for the simultaneous observations. The observed X-ray count rates were found to be 3.7 count s^{-1} on 1988 June 15 and 2.7 count s^{-1} on 1988 July 17 for the LAC effective area of 4000 cm^2 in the energy range 2–35 keV, although there is not a statistically significant number of photons in the energy range above 20 keV. The wide band count rates are summarized in Table 3.

In each observation, the X-ray detectors are positioned at the target for a day, and the background was measured at a sky location near BL Lacertae for a day on an adjacent day. The effective exposure time is ~ 14,000 s and ~ 16,000 s for the June and the July observations, respectively.

It is essential to obtain the data on the two occasions which can be compared with each other with little ambiguity. Great care has been taken to reduce the systematic errors, which are predominantly dependent on the estimation of the backgrounds.

First, we carefully estimated the non-X-ray background by two methods. One method uses the background sky observations taken on the adjacent day at satellite orbits with very similar background environments. The other employs the multiparameter fitting of the large data base of background observations (Hayashida et al. 1989). These two methods are found to give consistent values for the background. In addition, we used only the data taken from satellite orbits with stable background conditions, so that there is a small uncertainty in estimation of background induced by charged particles.

Secondly, the field of view (1° × 2° FWHM) of the two observations were chosen to cover the same region in the sky, in order to avoid the spatial fluctuation of the X-ray background. The center of the field of view was always set at BL Lacertae, and the position angle of the long axis of the field of view was set at a similar angle for the two observations. As a result, the difference in the region of the sky observed on two occasions is less than 10% of the field of view and is covered only with reduced sensitivity. Since the fluctuations of the X-ray background due to unresolved weak sources (confusion limit) is estimated to be 0.9 count s^{-1} rms for the LAC field of view (2–35 keV), the systematic offset between the counts detected in the two observations is estimated to be less than 0.1 count s^{-1} with more than 90% statistical confidence. The Poisson statistical errors in the count rates in Table 3, is, therefore, smaller than the fluctuation of background due to weak unresolved sources. The difference in the count rates between the two observations, in particular, is free from the spatial background fluctuations. The decrease of the X-ray intensity by 1.0 ± 0.1 counts s^{-1} was measured with good statistical confidence. The measured decrease in X-ray flux corresponds to 27% ± 7% of the flux on June 15, where the uncertainty arises from the uncertainty in the source flux due to unresolved sources. Observations taken on a single day are consistent with no variation, although because of low number statistics, variation of up to 30% on a time scale of hours cannot be ruled out.

The observed energy spectra are shown in Figure 2. These spectra were fitted by a simple power-law model with a low-energy cut-off due to a neutral absorption column. The best fit parameters are shown in Table 4. The spectral index for the two observations are apparently different. However, this result is sensitively dependent on the estimation of background in the high-energy range where the source flux is low. Consequently, the difference in the index may not have large significance.

The energy index at our two observations are consistent with the value obtained by the Einstein observations as a con-

---

NOTES TO TABLE 2

[a] In ergs cm^{-2} s^{-1} Hz^{-1} ($=10^{23}$ Jy). Corrected for $E(B-V) = 0.31$.
[b] In keV.
[c] In ergs cm^{-2} s^{-1} Hz^{-1}.
[d] Wavelength in angstroms.
[e] In ergs cm^{-2} s^{-1} Å^{-1}.
[f] Flux density in mJy.
[g] Magnitudes.

[h] Wavelength in μm.
[i] Magnitudes.
[j] Flux density in mJy.
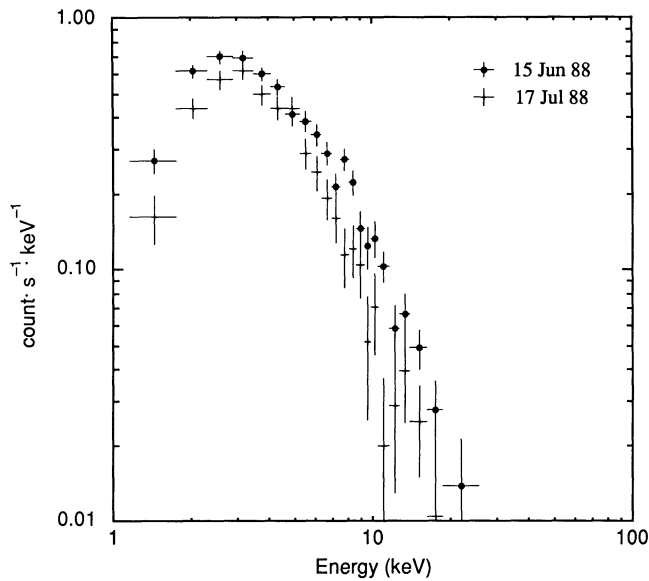[k] Flux density in Jy.
[l] Frequency in GHz.

FIG. 2.—X-ray Pulse height spectra of BL Lacertae at observations on 1988 June 15 and July 17.

FIG. 3.—Flux per logarithmic band width of BL Lacertae spectra taken in 1988 June and July.

necting slope between the MPC and IPC data ($\alpha = 0.68$; Bregman et al. 1990). Note that the *Einstein* index was obtained between energies 5.6 and 1.0 keV whereas the *Ginga* indices are determined in a much wider energy range 2–20 keV. The energy flux densities of the X-ray band shown in the wide band spectra (Fig. 1) are calculated from the best-fit power-law models. The comparison of the X-ray flux density with the *Einstein* IPC data and the *EXOSAT* LE data (Fig. 4) is made by extrapolating the power-law model.

2.2. *Multiwavelength Spectra*

As shown in Figure 1, there were no large differences in flux between the June and July observations except for ~30% flux decrease in X-ray. The multifrequency spectra, displayed as power per logarithmic bandwidth νF_ν versus $\log \nu$, are also shown in Figure 3 for the 1988 June and July data. The general feature of the spectra is unchanged from previous observations with a striking peak near $\log \nu = 14.3$, followed by remarkable steepening of the optical-ultraviolet continuum. The X-ray spectra lie clearly above an extension of the infrared-ultraviolet continuum, and its spectral slope is flatter than the optical-ultraviolet band and is rather similar to that of the far-infrared band. The separation of the X-ray emission from the radio-ultraviolet continuum suggests that it is caused either by a separate emission mechanism (e.g., the inverse Compton process), or by the synchrotron process, but in a region distinct from the radio-ultraviolet plasma. The information contained
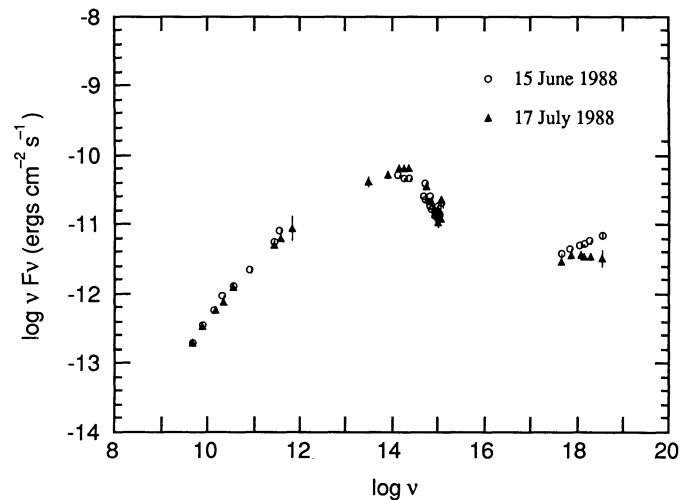
in the multifrequency spectra, when combined with variability data, can provide powerful constraints on the structure of the emitting region.

By comparing the various multifrequency spectra, variability as a function of wavelength can be explored, which is a critical test in understanding the connection between the different emitting regions. The variation between the 1988 June and July observations was reliably measured in the X-ray band, which showed the greatest relative change (a 30% decrease). For most of the other wavebands, a variation of this magnitude is easily ruled out at the 3 σ level. Smaller variations in the same sense as the X-ray data are seen in the radio waveband, which underwent a slow decrease in the total flux density and a more dramatic decrease in the polarized flux density (0.6–0.25 Jy) from 1988 March to August. This is weak evidence that radio emitting plasma and the X-ray emitting plasma may be related. However, upon comparing the 1988 data to previous multifrequency spectra (Bregman et al. 1990), much more dramatic changes are seen. The most important comparison is with the 1983 December spectrum (Fig. 4), in which both the radio-infrared and the X-ray fluxes are brighter while the optical-ultraviolet fluxes are dimmer. This suggests that the X-ray emission may be more closely related to the radio-infrared region than to the optical-ultraviolet region. This confirms the result obtained in an earlier effort (Bregman et al. 1990) in using the 1980 June and 1983 December multifrequency spectra. A comparison between the 1988 data and that of 1980 June is somewhat ambiguous because the latter spectrum is incomplete due to the lack of infrared data.

2.3. *Polarization*

Linear polarization measurements were obtained in the optical and radio regions during both the 1988 June and July dates (Table 5). In the optical waveband during 1988 June, the percentage polarization increased from 9% to 11% as the wavelength decreases from 6000 Å to 3500 Å, although the angle of polarization was nearly constant at ~20°. For the 1988 July optical measurements the percentage of optical polarization had hardly changed, but the angle of polarization had decreased by ~8°. The radio polarization measurements show significantly different polarization angles, but when corrected for the rotation measure of the galaxy, the polarization

TABLE 4
BEST-FIT SPECTRAL PARAMETERS FOR A POWER-LAW MODEL

Parameters	1988 June 15	1988 July 16
Norm	7.54 ± 0.82	11.8 ± 4.9
Photon Index	1.71 ± 0.07	2.16 ± 0.24
$\log N_H$	consistent with 0	21.9 ± 0.4

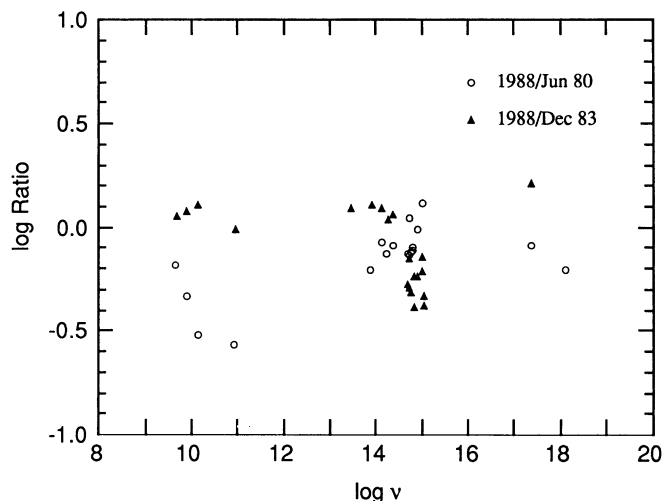NOTE.—Quoted uncertainties are 90% single-parameter confidence limits derived only from Poisson statistics

Fig. 4.—The multifrequecy flux ratio: the average flux of 1988 June and July observations is compared to that of the 1980 June observations, and to that of the 1983 December observations.

angle is nearly the same at all wavelengths and is near that of the 14.5 GHz point. The radio data show that the angle of polarization, like the optical data, decreased during this period by 12° at 14.5 GHz. In addition, the amount of polarization, 7%–11% and the angle of polarization, 20°–30°, is comparable to the optical values. The close relationship between the angle and degree of polarization indicates that the emission in these two wavebands come from a common structure, such as a jet, but most likely from different spatial locations.

3. DISCUSSION AND SUMMARY

The multifrequency observations presented here show that the power per logarithmic bandwidth is sharply peaked in the near infrared, with a precipitous decline in the optical-ultraviolet region and a slower decrease toward far-infrared and radio frequencies. Most of the power emerges in the 0.5–100 micron region. The X-ray emission from BL Lacertae is distinct from the emission at lower frequencies. There is neither a smooth connection between the X-ray and the optical-ultraviolet spectrum, nor are the slopes similar.

One of the reasons for obtaining these spectra was to test the

leading radiation models for these objects. The synchrotron-Compton model (Ghisellini, Maraschi, & Treves, 1985) predicts that the flux of the seed and Compton-scattered photons should change together. The spectral slope of the seed and the scattered photons should be the same. If we identify the X-ray photons as the scattered photons, then the seed photon would be identified with the infrared-submillimeter region by this argument. The X-ray and infrared-submillimeter regions were found to vary together, which supports the expectation of the synchrotron-Compton model. We note that our data are in apparent conflict with certain simple versions of the pair cascade model, in which soft optical and ultraviolet photons are scattered into the X-ray region. In this model, one might expect that the optical-ultraviolet continuum would be correlated with the X-ray emission, which it is not. The data presented here provide the most detailed test to date of these radiation models. In previous efforts, either the X-ray slope was unknown, the multifrequency spectra were incomplete, the variability data was inadequate, or the X-ray continuum was not distinct from the lower frequency emission.

From the variability behavior coupled with the continuum shape, BL Lacertae is unique in that it provides the strongest support to the synchrotron self-Compton model. In other objects that have been observed, the X-ray emission is sometimes an extension of the optical-ultraviolet emission, such as for PKS 2155−304 (Urry 1986; Ohashi et al. 1989), and therefore is probably produced by the synchrotron process. In other objects, the X-ray emission may appear distinct from the optical emission (e.g., 3C 446; Bregman et al. 1986), but vary together with it, which is not what would be expected from the familiar synchrotron self-Compton model. Because of its special behavior and relative brightness, BL Lacertae is the ideal object in which to further investigate the inverse Compton mechanism. Basic questions still need to be answered, such as the size of the X-ray–emitting region (possible to accomplish through variability studies) and whether short-term variations in the X-ray and infrared region are connected.

TABLE 5

POLARIZATION DATA FOR BL LACERTAE, 1988 JUNE/JULY

Observer	Date (1988)	Wave	log ν	Polarization (%)	Position Angle
Miller and Goodrich	Jun 15	3500	14.933	10.90	17.6
		4000	14.875	10.66	20.4
		4500	14.824	10.79	21.3
		5000	14.778	9.95	19.7
		5500	14.737	9.00	20.4
		6000	14.699	8.95	19.7
Wills and Wills	Jul 15	4400	14.834	9.49	11.8
	Jul 17	4400	14.834	10.45	12.5
Aller, Aller, and Hughes	Jun 15	14.5	10.161	8.00	30.0
		8.0	9.903	8.30	16.0
		4.8	9.681	10.70	−9.3
	Jul 17	14.5	10.161	6.60	18.0
		8.0	9.903	7.00	11.0
		4.8	9.681	9.20	−10.1

REFERENCES

Bregman, J. N., Maraschi, L., & Urry, C. M. 1987, in Scientific Accomplishments of the *IUE*, ed. Y. Kondo (Dordrecht: Reidel), 685
Bregman, J. N., et al. 1990, ApJ, 352, 574
Ghisellini, G., Maraschi, L., & Treves, A. 1985, A&A, 146, 204
Gould, R. J. 1979, A&A, 76, 306
Guilbert, P. W., Fabian, A. C., & Rees, M. J. 1983, MNRAS, 205, 593
Hayashida, K. et al. 1989, PASJ, 41, 373
Jones, T. W., O'Dell, S. L., & Stein, W. A. 1974, ApJ, 188, 353
Makino, F., et al. 1987, ApJ, 313, 662

Miller, J. S. French, H. B., & Hawley, S. A. 1978, ApJ, 219, L85
Ohashi, T., et al. 1989, PASJ, 41, 709
Svensson, R. 1987, MNRAS, 227, 403
Turner, M. J. L., et al. 1989, PASJ, 41, 345
Urry, M. C. 1986, in The Physics of Accretion onto Compact Objects, ed. K. O. Mason, M. G. Watson, & N. E. White (Berlin: Springer-Verlag), 357
———. 1988, in Multiwavelength Astrophysics, ed. F. A. Córdova (Cambridge University Press), 279